

The KRAB-containing zinc-finger transcriptional regulator ZBRK1 activates SCA2 gene transcription through direct interaction with its gene product, ataxin-2

Linda Hallen^{1,2}, Holger Klein¹, Carola Stoschek¹, Silke Wehrmeyer¹, Ute Nonhoff^{1,†}, Markus Ralser¹, Jeannine Wilde¹, Christina Röhr^{1,2}, Michal R. Schweiger¹, Kurt Zatloukal³, Martin Vingron¹, Hans Lehrach¹, Zoltán Konthur¹ and Sylvia Krobitsch^{1,*}

¹Max Planck Institute for Molecular Genetics, Ihnestr. 73, 14195 Berlin, Germany, ²Department of Biology, Chemistry and Pharmacy, Free University Berlin, Takustr. 3, 14195 Berlin, Germany and ³Medical University of Graz, Auenbruggerplatz 25, 8036 Graz, Austria

Received August 13, 2010; Revised and Accepted October 3, 2010

Gene transcription is controlled by transcriptional regulators acting with specific co-regulators to allow gene activation and repression. Here, we report the identification of the KRAB-containing zinc-finger transcriptional regulator, ZBRK1, as an interaction partner of the SCA2 gene product ataxin-2. Furthermore, we discovered that an elevated ZBRK1 level resulted in increased ataxin-2 levels, whereas interference on transcriptional and protein levels of ZBRK1 yielded reduced ataxin-2 levels, suggesting that a complex comprising ZBRK1 and ataxin-2 regulates SCA2 gene transcription. A bioinformatic analysis utilizing the known ZBRK1 consensus DNA-binding motif revealed ZBRK1-binding sites in the SCA2 promoter. These predicted sites were experimentally validated by chromatin-immunoprecipitation experiments along with luciferase-based promoter analyses corroborating that SCA2 gene transcription is controlled by a ZBRK1/ataxin-2 complex. Finally, we demonstrate that SCA2 gene transcription is significantly reduced in colon tumors possessing low ZBRK1 transcripts. Thus, our results provide first evidence that ataxin-2 acts as a co-regulator of ZBRK1 activating its own transcription, thereby representing the first identified ZBRK1 co-activator.

INTRODUCTION

Krüppel-associated box (KRAB)-containing zinc-finger repressor proteins represent the largest single family of transcriptional regulators accounting for approximately one-third of the different zinc-finger proteins present in the human genome. Members of this family are involved in the transcriptional repression of RNA polymerase I, II and III promoters, as well as binding and splicing of RNA, resulting in crucial functions regarding the maintenance of the nucleolus, cell differentiation and proliferation and apoptosis. However, for most members, the cellular function and the underlying molecular mechanisms remain elusive (1–3).

The zinc-finger protein 350 (ZNF350), also known as BRCA1-interacting protein with a KRAB domain 1 (ZBRK1), was initially isolated in a yeast two-hybrid (Y2H) screen carried out to identify proteins associated with the breast-cancer-associated protein 1 (BRCA1) (4). ZBRK1 is a nuclear protein with a molecular mass of 60 kDa that is ubiquitously expressed. From structural scrutiny, ZBRK1 comprises a highly conserved KRAB domain at the N-terminal region consisting of two KRAB boxes, KRAB A and KRAB B, which act generally as a transcriptional repressor domain through association with co-repressor proteins (3). The KRAB A box plays a key role in repression mediated by binding to co-repressors, enhanced by KRAB B through yet unknown mechanisms (5). Further, ZBRK1 encompasses

*To whom correspondence should be addressed. Tel: +49 3084131351; Fax: +49 3084131960; Email: krobitsc@molgen.mpg.de

†Present address: UGA Biopharma GmbH, Neuendorfstr. 20a, 16761 Hennigsdorf, Germany.

eight consecutive Krüppel-type C2H2 zinc-finger motifs in the central region, which are responsible for DNA binding, and the BRCA1-binding domain, termed CTRD, in the C-terminal region, which serves as a protein–protein interaction surface controlling ZBRK1-directed transcriptional regulation (6,7).

As to ZBRK1 function, a link to the cellular DNA damage repair response has been provided by demonstrating that ZBRK1 binds to the DNA recognition motif GGGnnnCAGnnnTTT within intron 3 of the DNA damage-responsive *GADD45* gene (growth arrest and DNA damage gene 45), thereby repressing transcription in a BRCA1-dependent manner (8). Upon treatment of mammalian cells with ultraviolet light or DNA-damaging agents such as methyl methanesulfonate, ZBRK1 is rapidly degraded through the ubiquitin–proteasome pathway and consequently transcription of the *GADD45* gene is induced. Besides, ZBRK1 overexpression caused a decrease in both *GADD45* transcripts and protein (8). Since the ZBRK1 DNA recognition motif has been found in several BRCA1-targeted genes, a common function of ZBRK1 in response to DNA damage has been proposed (4).

In addition to this, ZBRK1 is implicated in the tumorigenesis of several human cancers. A repressor complex consisting of ZBRK1, BRCA1 and CtIP (CtBP-interacting protein) has been identified on the angiopoietin-1 promoter bound through the ZBRK1 DNA recognition motif (9). Depleting this complex paralleled with increased angiopoietin-1 expression accelerating mammary tumor growth due to prominent vasculature formation. Moreover, alterations in *ZBRK1* gene expression occur quite frequently in breast and colon carcinomas, with a tendency to ZBRK1 under-representation in both (10,11). Low *ZBRK1* transcripts have been also discovered in cervical tumor cells (12). Interestingly, increased ZBRK1 levels inhibited malignant growth, invasion and metastasis in cervical cancer cells, indicating that ZBRK1 acts as metastatic suppressor. Elevated ZBRK1 levels resulted in a significant upregulation of 23 genes, for example, *ZNF467* (zinc-finger protein 467), *VIM* (vimentin), *SH3GLB2* (SH3-domain GRB2-like endophilin B2) or *NCAM1* (neural cell adhesion molecule 1), which function in cellular movement, gene expression as well as cellular growth and proliferation. These observations propose that ZBRK1 does not solely function as a transcriptional repressor and suggest the existence of potential, yet unknown, co-activators (12).

In this study, we report an interaction between ZBRK1 and the *SCA2* gene product ataxin-2 (ATXN2), which is implicated in the polyglutamine disorder spinocerebellar ataxia type 2 (SCA2), and has been linked to functions in cellular RNA metabolism and endocytotic processes (13–17). Moreover, we provide evidence that a complex comprising ZBRK1 and ATXN2 is regulating *SCA2* gene transcription. ZBRK1 overexpression led to an increase in ATXN2 levels, whereas lowering ZBRK1 levels resulted in reduced levels. Finally, the application of an intrabody with interfering properties for this interaction further corroborated that a complex comprising ZBRK1 and ATXN2 is regulating *SCA2* gene transcription. A bioinformatic analysis predicted ZBRK1-binding sites (ZBSs) within the *SCA2* promoter, which were

experimentally validated by chromatin-immunoprecipitation (ChIP) experiments and promoter analyses. Of note, we demonstrate that in colon tumors *SCA2* gene transcription is significantly reduced and is correlated to low *ZBRK1* transcripts. Taking all results into consideration, this is the first report linking ATXN2 to transcriptional regulation by demonstrating that ATXN2 functions as a co-regulator of ZBRK1 activating its own transcription.

RESULTS

The KRAB-containing zinc-finger transcriptional regulator ZBRK1 interacts with ATXN2

Over the last years, evidence has been provided that ATXN2 functions in cellular RNA metabolism and endocytotic processes (13–17). In order to gain further insights into its cellular functions, we carried out a Y2H screen with the LSm domain of ATXN2 as bait protein using as prey a human fetal brain library (Clontech). In this screen, nine yeast clones were initially isolated from 2×10^5 transformants. From these, only two clones were confirmed as positive prey clones by independent Y2H experiments and sequencing analysis, of which one encodes for part of the C-terminal region of the KRAB-containing zinc-finger transcriptional regulator ZBRK1 (Fig. 1A, left panel). Subsequently, we performed further Y2H analyses using bait plasmids encoding different ATXN2 regions as illustrated (Fig. 1A, right panel) and the isolated prey plasmid encoding the fusion protein AD-ZBRK1_{234–532}. This analysis revealed that the activity of reporter genes of yeast cells expressing the fusion proteins LexA-ATXN2(Q22)_{1–396}, representing the N-terminal region of ATXN2 comprising part of the LSm domain, and AD-ZBRK1_{234–532} is stronger compared with yeast cells expressing the fusion proteins LexA-ATXN2_{254–475} and AD-ZBRK1_{234–532} (Fig. 1B, left and middle panel). To verify specificity of this interaction, we included two other glutamine-rich proteins, huntingtin (HDQ25) and ataxin-3 (ATXN3), as unrelated bait proteins in this study. No reporter gene activity was observed in yeast cells expressing LexA-HDQ25 and AD-ZBRK1_{234–532} or LexA-ATXN3 and AD-ZBRK1_{234–532}, respectively (Fig. 1B, right panel), indicating that the observed interaction between the C-terminal region of ZBRK1 and ATXN2 is specific in the Y2H system.

Next, we investigated whether this interaction occurs in mammalian cells as well. One obstacle here is the relatively low endogenous ZBRK1 level in a high number of human cell lines according to the human protein atlas (<http://www.proteinatlas.org>). Therefore, we first carried out co-immunoprecipitation experiments by transfecting cells with the expression plasmid pTL-FLAG-ZBRK1 or pTL-FLAG as a control. Cells were lysed and processed as described in Materials and Methods. As shown in Figure 1C, FLAG-tagged ZBRK1 was precipitated with an antibody directed against ATXN2; no protein was precipitated from the control lysate. By confocal microscopy, we were able to detect a nuclear localization of transiently overexpressed ZBRK1 and endogenous ATXN2 next to its cytoplasmic

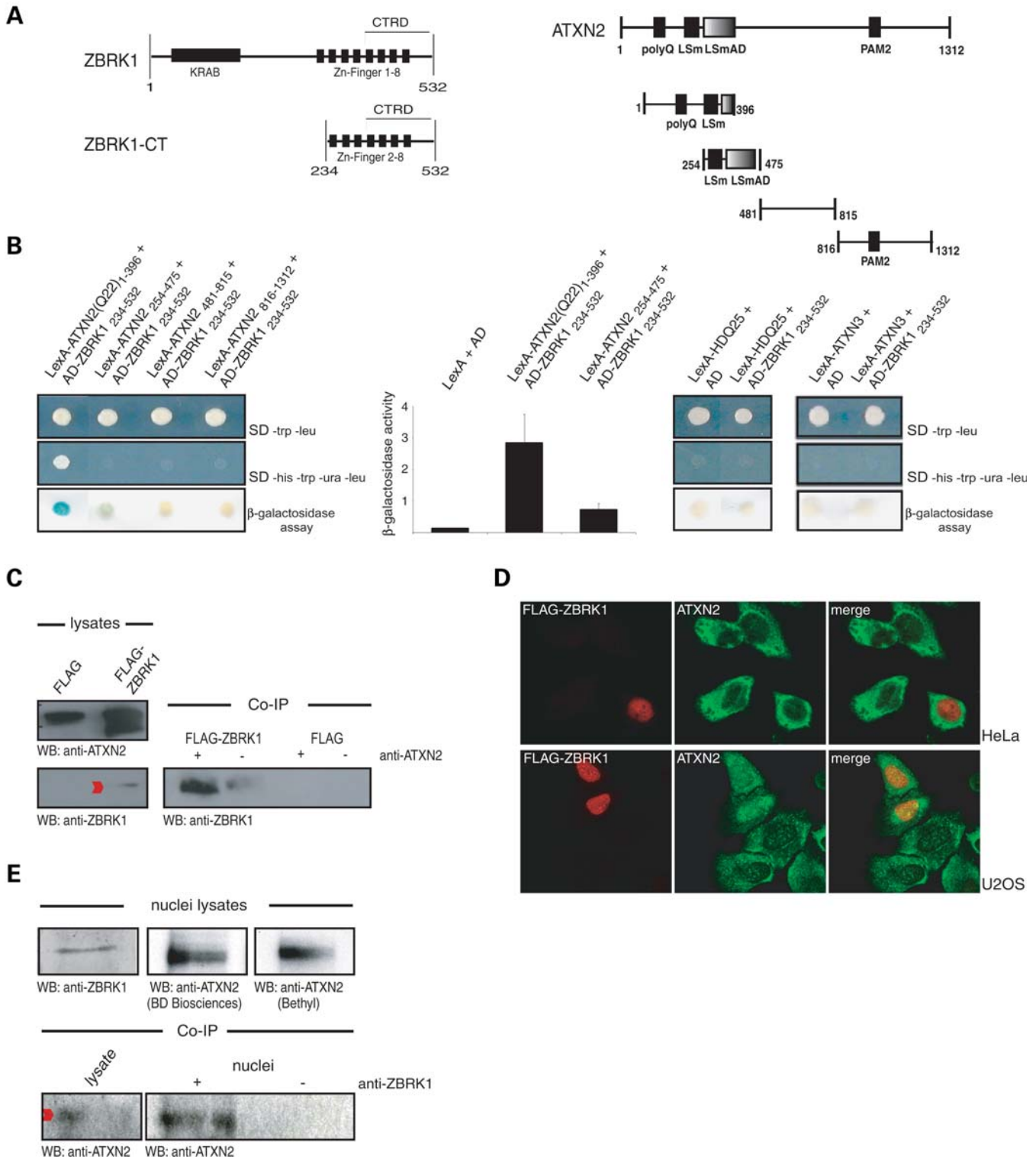


Figure 1. The transcriptional regulator ZBRK1 interacts with ATXN2. **(A)** Schematic illustration of ZBRK1 and ATXN2 and regions thereof used in the Y2H system. The oblongs represent the KRAB domain and the zinc fingers within ZBRK1 (left panel) or the polyglutamine domain with 22 glutamines (polyQ), the LSm and LSmAD domain and the PAM2 motif within ATXN2 (right panel). **(B)** Yeast strain L40ccua was co-transformed with the relevant bait and prey plasmids, and transformants were selected and spotted onto selective media or membrane to analyze the activity of the reporter genes. *LacZ* reporter activity was also determined by liquid β -galactosidase assay. **(C)** Co-immunoprecipitation experiments. Hek293T cells were transfected with plasmid pTL-FLAG-ZBRK1 or pTL-FLAG as a control. Cell lysates were incubated with an antibody directed against ATXN2 and precipitated proteins were visualized as indicated. **(D)** Confocal microscopy. HeLa and U2OS cells were transiently transfected with plasmid pTL-FLAG-ZBRK1. Sixteen hours post-transfection cells were fixed and stained with specific antibodies for ATXN2 and FLAG-tag. **(E)** Detection of endogenous ZBRK1 and ATXN2 in HeLa nuclei extract using an antibody against ZBRK1 and two different antibodies directed against ATXN2 (upper panel). Co-immunoprecipitation of ATXN2 from HeLa nuclei extract with an antibody directed against ZBRK1. Detection with ATXN2 antibody (BD Biosciences) (lower panel).

localization in HeLa and U2OS cells, which have been utilized in functional ZBRK1 characterization studies (4,8,12) (Fig. 1D). Therefore, we carried out additional co-immunoprecipitation experiments using commercially available HeLa nuclei extracts. Endogenous ATXN2 was precipitated from nuclei extracts using an antibody directed against endogenous ZBRK1 (Fig. 1E). Thus, these experiments demonstrate that an association between ZBRK1 and ATXN2 takes place in mammalian cells.

SCA2 gene transcription is coordinated by a ZBRK1/ATXN2 complex

Some cells transiently overexpressing ZBRK1 seem to exhibit a higher cellular ATXN2 immunoreactivity compared with non-transfected cells (Fig. 1D). We therefore transfected Hek293T cells with plasmid pCMV-MYC-ZBRK1 or control vector pCMV-MYC to determine the protein levels of ATXN2 in the presence of elevated ZBRK1 levels. Cells were lysed 48 h post-transfection and lysates were subjected to sodium dodecyl sulphate–polyacrylamide gel electrophoresis (SDS–PAGE) and western blotting. As shown in Figure 2A, cell lysates derived from cells transiently overexpressing ZBRK1 exhibited an elevated ATXN2 level in comparison to control lysates. We also investigated the effect of ZBRK1 depletion on the *SCA2* gene product by RNA interference experiments as well. For these, Hek293T cells were transfected with siRNA molecules specific for ZBRK1 as well as unspecific siRNA as a control. As analyzed by reverse transcription–quantitative real-time PCR (RT–qPCR), treatment of cells with ZBRK1-specific siRNA resulted in a ZBRK1 knockdown efficiency of 60–65% (data not shown). As expected, the endogenous ATXN2 level in lysates of ZBRK1-depleted cells was reduced in comparison to respective control cell lysates (Fig. 2B). Finally, we generated and applied an intrabody with interfering properties for this interaction following an approach as described in Materials and Methods. Expression of this intrabody in mammalian cells and subsequent immunoprecipitation experiments revealed that this intrabody precipitated endogenous ZBRK1, indicating specificity (Fig. 2C, upper panel). Interestingly, we observed that the expression of this intrabody resulted in lowered ATXN2 levels than expression of a control intrabody (Fig. 2C, lower panel). Thus, our results suggest that a complex comprising ZBRK1 and ATXN2 regulates *SCA2* gene transcription and consequently ATXN2 levels.

The *SCA2* promoter comprises ZBRK1-binding motifs

In order to corroborate the assumption that ZBRK1 and ATXN2 are coordinately regulating *SCA2* gene transcription, we subsequently performed a *SCA2* promoter analysis exploiting the annotated ZBRK1-binding motif GGGnnnCAGnnnTTT. This motif was originally identified by sampling a random pool of double-stranded oligonucleotides with recombinant ZBRK1 lacking the C-terminal region that is important for the oligomerization of ZBRK1 (4). Notably, the search for occurrences of the International Union of Pure and Applied Chemistry (IUPAC) string GGGnnnCAGnnnTTT or its reverse complement allowing up to three mismatches in the outer two nucleotide triplets

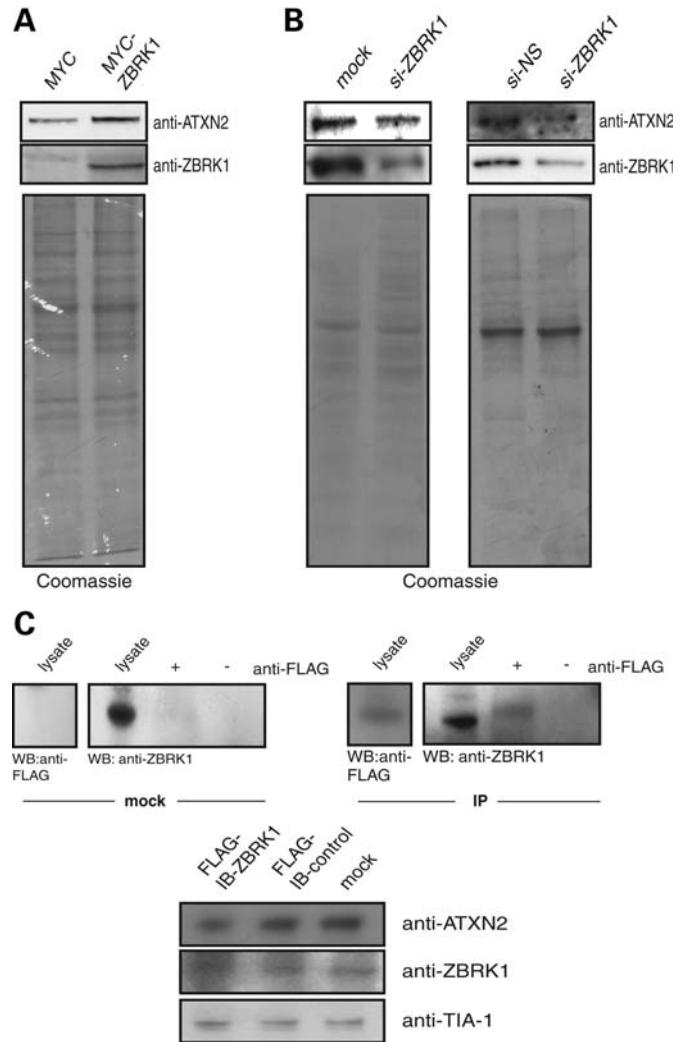


Figure 2. Expression of the *SCA2* gene product is regulated by a ZBRK1/ATXN2 complex. (A) ZBRK1 overexpression experiments. Hek293T cells were transfected with pCMV-MYC-ZBRK1 or control vector and lysed 48 h post-transfection. Proteins were visualized with antibodies as indicated. Coomassie-stained gels served as loading controls. (B) Knockdown experiments. Hek293T cells were transfected with unspecific or ZBRK1-specific siRNA or left untreated. Then, cells were incubated for 96 h, lysed and protein levels were analyzed by immunoblotting. Coomassie-stained gels served as loading controls. (C) Immunoprecipitation experiments. Hek293T cells expressing FLAG-ZBRK1 intrabody or control cells were lysed and incubated with an antibody directed against the FLAG-tag. Precipitated ZBRK1 was visualized by a ZBRK1 antibody (upper panel). Interference experiments. Hek293T cells were transfected with the respective intrabody plasmid or a control intrabody plasmid. Sixteen hours post-transfection, lysates were prepared and subjected to immunoblotting analysis. As the internal loading control, TIA-1 levels were used (lower panel). All experiments have been performed at least two times obtaining the same results.

resulted in the identification of seven putative ZBSs within the analyzed *SCA2* sequence region (Fig. 3A, left panel). To validate these experimentally, we performed ChIP experiments focussing on four predicted sites: ZBS1 and ZBS2, which are located near the transcriptional start site (TSS) and partly overlap; ZBS3, which is located in a non-conserved region of the *SCA2* promoter, as well as ZBS4, which is located in the coding sequence of exon 1 of the *SCA2* gene. Cells were crosslinked with formaldehyde,

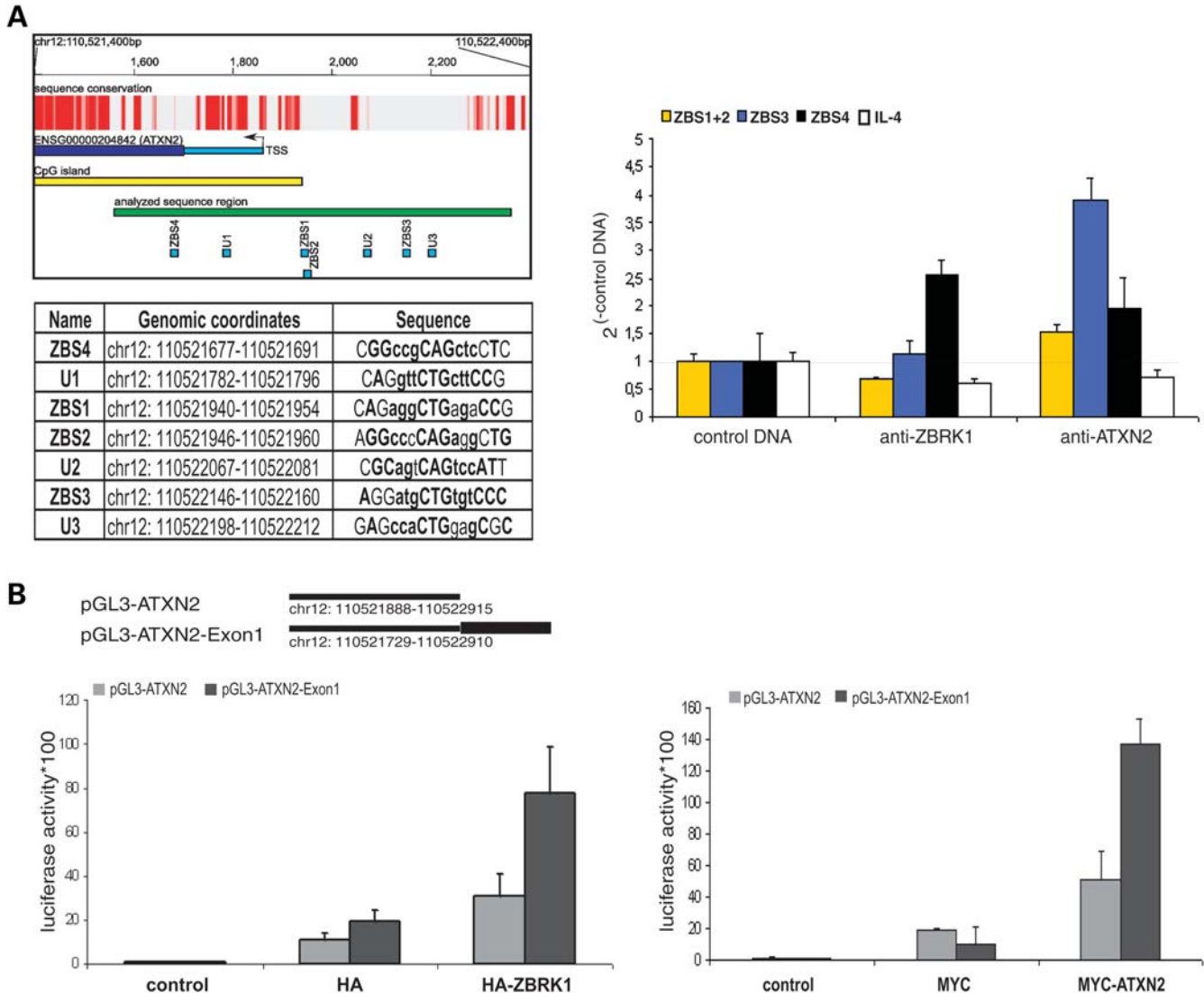


Figure 3. ZBRK1 binds the *SCA2* promoter through internal ZBSs. (A) Illustration of the genomic location of the *SCA2* promoter relative to Ensembl 46/NCBI36. PHASTCONS 44-way vertebrate sequence conservation was imported from UCSC browser (35), with conserved regions shown in red. Regions of the analyzed *SCA2* sequence region are shown in green, exon 1 of the *SCA2* gene is shown in blue and the UTR in turquoise. CpG island (yellow) location was defined with method of Gardiner-Garden and Frommer (36). Putative ZBSs are depicted in turquoise. Binding sites chosen for ChIP experiments were named ZBS1–4, uncharacterized were named U1–3. Genomic coordinates are relative to Ensembl 46/NCBI36 (upper left panel). Putative ZBSs within the analyzed *SCA2* sequence region. Capitalized bases in the sequence correspond to conserved positions in the ZBRK1 SELEX set (lower left panel). Positions are marked in bold if the respective nucleotide occurs at least once in this position in a sequence from the SELEX set. ChIP experiments. MCF-7 cells were lysed and chromatin DNA was immunoprecipitated with antibodies directed against ZBRK1 or ATXN2, validated by qPCR using primers encompassing the predicted ZBSs and normalized to control DNA. The chromosomal region of IL-4 (chr5:132037145–132037263) served as a negative control. Bars indicate the standard error of the mean (right panel). (B) Schematic illustration of the *SCA2* reporter constructs pGL3-ATXN2 (chr12:110521888-110522915) and pGL3-ATXN2-Exon1 (chr12:110521729-110522910) (upper left panel). Promotor analysis. Hek293T cells were transfected with plasmids pGL3-ATXN2 or pGL3-ATXN2-Exon1, plasmid pRL-TK-Renilla and plasmid pCMV-HA-ZBRK1 or empty vector or pCMV-MYC-ATXN2-Q22 or empty vector, respectively. Twenty-four hours post-transfection, cells were lysed, the expression of *Firefly* and *Renilla* luciferase were measured and their ratios were set in relation to pGL3basic.

lyzed and nuclei were isolated. After sonification of genomic DNA, samples were incubated with an antibody against ZBRK1 or ATXN2. Precipitated DNA fragments were analyzed by RT-qPCR using primers encompassing a ~120 bp fragment around the predicted ZBRK1-binding motifs. Using an antibody directed against ZBRK1, we were able to precipitate and highly enrich DNA fragments containing the ZBRK1-binding motif ZBS4 (Fig. 3A, right panel). Moreover, DNA fragments containing ZBS3 were precipitated; however, enrichment was weak. No enrichment was observed for ZBRK1-binding motifs ZBS1 and

ZBS2. Nonetheless, all four ZBRK1-binding motifs were precipitated and significantly enriched with an antibody directed against ATXN2 (Fig. 3A, right panel). Thus, we concluded that ZBRK1 and ATXN2 form a complex bound to the ZBSs within the *SCA2* promoter regulating *SCA2* gene transcription.

To sustain this finding, we carried out additional promoter studies. For these, we generated Firefly expression plasmids pGL3-ATXN2 containing *SCA2* promoter sequences comprising the ZBS1–3 and pGL3-ATXN2-Exon1 containing *SCA2* promoter sequences comprising all predicted ZBSs

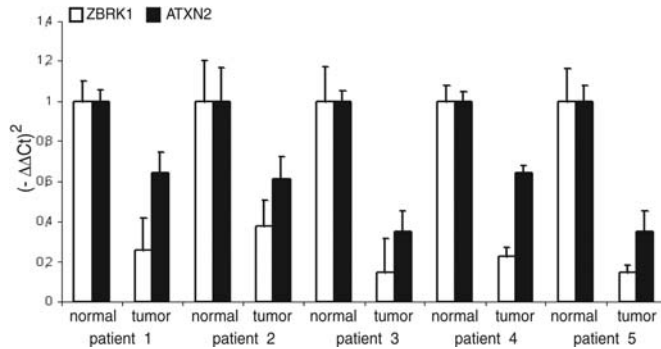


Figure 4. *SCA2* gene transcription is reduced and correlates with low *ZBRK1* transcripts in colon cancer patient tissue. RT-qPCR analysis. Isolated RNA from matching normal and tumor tissues of five colon cancer patients were analyzed by RT-qPCR. Bars indicate the standard error of the mean.

(Fig. 3B, upper left panel). Hek293T cells were transiently transfected with plasmids pGL3-ATXN2 or pGL3-ATXN2-Exon1, plasmid pRL-TK-Renilla encoding *Renilla* luciferase and plasmid pCMV-HA-ZBRK1 or empty vector, respectively, as indicated. After transfection, cells were lysed and expression of *Firefly* and *Renilla* luciferase was measured and their ratios were set in relation to pGL3basic. As shown in Figure 3B, *ZBRK1* overexpression led to an increase in *SCA2* promoter activity that was stronger in case all ZBSs were present (left panel). On the other hand, the same set of experiments was performed with cells transiently overexpressing *ATXN2*. As observed for *ZBRK1*, elevated *ATXN2* levels resulted in enhanced *SCA2* promoter activity as well (Fig. 3B, right panel). Taking all these results into consideration, we concluded that *ZBRK1* acts as an activator on *SCA2* gene transcription and that *ATXN2* represents a co-regulator, most probably a co-activator, regulating its transcription through complex formation with *ZBRK1*.

***ATXN2* transcripts are reduced in colon cancer patient material with low *ZBRK1* transcripts**

Since low *ZBRK1* expression has been observed in diverse human carcinomas, e.g. in 50% of hepatocellular carcinomas and 37.5% of colorectal cancers (10–12), we finally set out to investigate whether the observed correlation between *ZBRK1* and *ATXN2* *in vitro* is also reflected at the transcriptional level in cancer tissues. Samples of matching normal and tumor tissues of five colon cancer patients were collected, macrodissected and transcriptional levels of *ZBRK1* and *SCA2* gene were determined by quantitative RT-qPCR. As expected, all colon tumor tissues showed a decrease in *ZBRK1* transcripts in comparison to their normal counterparts (Fig. 4). In addition, reduced *SCA2* gene transcripts were detected in all tumor tissues compared with their normal counterparts as well. Taken together, these results draw a parallel with the observations made in our cell culture experiments demonstrating a correlation between *ZBRK1* and *SCA2* gene transcription further strengthening the assumption that a complex comprising *ZBRK1* and *ATXN2* regulates *SCA2* gene transcription.

DISCUSSION

In this study, we report for the first time on an interaction between the transcriptional regulator *ZBRK1* and *ATXN2*. This interaction occurs with the C-terminal region of *ZBRK1* that mainly consist of the BRCA1-binding domain, termed CTRD. Of note, this domain has been shown to be responsible for tetrameric oligomerization of *ZBRK1* assembling on *ZBRK1* DNA consensus motifs and thus facilitating *ZBRK1*-directed transcriptional repression (7). Additionally, evidence has been provided that the regulatory potential of *ZBRK1* on certain target genes may also derive from its recruitment via CTRD-dependent protein–protein interactions rather than protein–DNA interactions (7); for example, binding of the tumor suppressor BRCA1 to CTRD is responsible for BRCA1-dependent transcriptional repression of several DNA damage-response genes (4). However, a role for additional co-regulators of the CTRD domain has been proposed mainly based on the observation that binding of BRCA1 is necessary, however not sufficient for *ZBRK1* repression function (7). In this regard, the transcription factors serum response factor (SRF) and activating transcription factor 1 (ATF-1) were found to bind to the CTRD domain in the Y2H system, however, further investigations have not yet been reported (7). Based on our finding, we propose that *ATXN2* also acts through its binding to the CTRD, representing a novel co-regulator of *ZBRK1*. We discovered potential ZBSs in the *SCA2* promoter and experimentally verified them by ChIP experiments further demonstrating that *ATXN2* is found in a complex with *ZBRK1* bound to the promoter. We suggest that *ATXN2* acts through its interaction with sequence-specific DNA binding transcription factors as it has been described for BRCA1 that is involved in both activation and repression of gene transcription through its direct interaction with several DNA-binding transcription factors (6,18–21). To this point, *ATXN2* function was previously linked to roles in the cellular RNA metabolism and endocytotic processes (13–17). However, this is the first report providing evidence that *ATXN2* is implicated in transcriptional regulation.

Furthermore, we demonstrate that a complex comprising *ZBRK1* and *ATXN2* is activating the transcription of the *SCA2* gene itself, thus suggesting that *ATXN2* functions as co-activator of *ZBRK1*. Transient *ZBRK1* overexpression resulted in increased *ATXN2* protein levels, whereas *ZBRK1* depletion or interaction interference resulted in reduced *ATXN2* levels. Moreover, increased *SCA2* promoter activity was found in the case of elevated *ZBRK1* or *ATXN2* levels. Although *ZBRK1* and other KRAB-containing zinc-finger proteins are thought to function mainly as transcriptional repressors, a dual function in gene repression and activation has been reported recently. Global expression profiling of HeLa or U2OS cells stably overexpressing *ZBRK1* clearly demonstrated the transcriptional activation of numerous genes, however, by yet unknown mechanisms and co-activators (12). Moreover, depletion of the KRAB-containing zinc-finger protein ZNF263 showed that this transcriptional regulator has activating as well as repressing effects on target gene transcription (22).

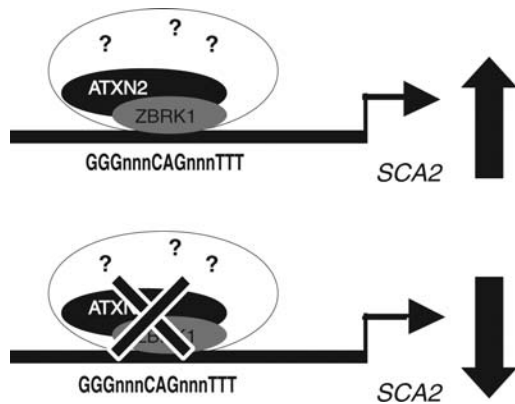


Figure 5. Schematic model for *SCA2* transcriptional regulation by ZBRK1/ATXN2 complex.

Alterations in *ZBRK1* gene expression have been frequently observed in human carcinomas, with a tendency to *ZBRK1* under-representation (10–12). We observed that low *ZBRK1* transcripts in colon cancer tissues correlate with low *SCA2* gene transcripts when compared with matching control colon tissue. In this regard, low ATXN2 levels have been linked to poor outcome of human neuroblastoma cells, a highly heterogeneous tumor of young children, whereas enforced expression of ATXN2 levels sensitizes neuroblastoma cells for apoptosis (23). Hence, it is tempting to speculate that the deregulation of ATXN2 is due to impairment in the ZBRK1/ATXN2 complex as it is for colorectal cancers, where we have selected advanced colorectal cancer cases with a metastatic disease.

As illustrated in Figure 5, deciphering the role of ATXN2 in transcriptional regulation and its potential function as the co-activator of ZBRK1, identifying additional components of the ATXN2/ZBRK1 complex and how alterations of the ATXN2/ZBRK1 complex affect target genes will be an interesting task to address in the future perspective.

Besides ATXN2's potential impact in tumorigenesis, one should keep in mind that ATXN2 has been linked to the neurodegenerative disorder SCA2, which is characterized by expansion of the trinucleotide repeat CAG in the *SCA2* gene encoding an enlarged polyglutamine region within ATXN2 (24–26). Remarkably, evidence has been provided that the accumulation of disease ATXN2 is contributing to cellular dysfunction, and finally SCA2 pathogenesis (27). Although tumorigenesis and neurodegeneration are different pathologies, common factors and overlapping pathways were identified over the last years, interestingly, often with complementary relationships. In this perspective, it will be of interest to study the effect of an expanded glutamine region within ATXN2 in regard to the interaction with ZBRK1 and the resulting consequences. Notably, first Y2H results indicate that the interaction between ATXN2 and ZBRK1 is affected in the disease state. Deciphering the resulting consequences of an altered ATXN2/ZBRK1 complex formation and how this contributes to SCA2 pathogenesis will be tremendously helpful in defining

the role of ATXN2 and ZBRK1 in the pathogenesis of SCA2.

MATERIALS AND METHODS

Plasmids

The Y2H bait plasmids used and the mammalian expression plasmid pCMV-MYC-ATXN2-Q22 were described earlier (14,16–17). To generate the mammalian expression plasmid pCMV-MYC-ZBRK1, the open-reading frame of the *ZBRK1* gene was amplified via PCR using plasmid pOTB7-ZBRK1 (RZPD, IRAUp969A0148D) as the template DNA and the oligonucleotide pair ZBRK1-s-SalI and ZBRK1-as-NotI. The resulting DNA fragment was treated with the restriction endonucleases *SalI/NotI* and subcloned into the *SalI/NotI* sites of the vector pCMV-MYC. Plasmids pCMV-HA-ZBRK1 and pTL-FLAG-ZBRK1 were created by subcloning the *SalI/NotI* DNA fragment from pCMV-MYC-ZBRK1 into the *SalI/NotI* sites of the vector pCMV-HA or the *XhoI/NotI* sites of the vector pTL-FLAG, respectively.

The *SCA2* promoter constructs, pGL3-ATXN2 and pGL3-ATXN2-Exon1, were amplified by PCR using genomic SW480 DNA and primer pair pGL3-ATXN2-FW and pGL3-ATXN2-RV or pGL3-ATXN2-Exon1-FW and pGL3-ATXN2-Exon1-RV, respectively. Subsequently, the amplified promoter regions were subcloned into the pGL3basic vector by Gateway BP clonase (Invitrogen) as recommended by the manufacturer. All DNA fragments were validated by sequencing. Primers are listed in Table 1. Underlined sequences represent restriction sites.

Y2H analysis

Y2H analyses were performed as described previously using the yeast strain L40ccua (16,17,28). After transformation of the respective bait and prey plasmids, the yeast transformants were isolated and single clones were spotted onto solid selective SD media lacking tryptophan, leucine (SDII) or SD media lacking tryptophan, leucine, uracil and histidine (SDIV) as well as on nylon membrane (MSI). After 3–5 days, growth of yeast on selective media was monitored. To analyze the activity of the *LacZ* reporter gene, the membrane was incubated in liquid nitrogen and incubated on Whatman paper that has been saturated with X-Gal buffer [phosphate buffer pH 7.0, 0.15% X-Gal (bromo-chloro-indolyl-galactopyranoside), 10 mM DTT] for 6–8 h at 37°C. The liquid β -galactosidase assay was performed as described (16).

Cell cultivation and transfection

MCF-7, U2OS, HeLa and Hek293T cells were cultivated in Dulbecco's modified Eagle's medium (Invitrogen) supplemented with 10% heat-inactivated fetal calf serum (Biocrom) and 1% penicillin/G-streptomycin (Biocrom) at 37°C and 5% CO₂. For overexpression studies, cells were plated on adequate plates and grown until a confluence of 50–70%. Transfections were performed with polyethylenimine (PEI; Polysciences).

Table 1. Primers used in this study

Primer	Sequence
ZBRK1-s-SalI	5'-GAGTCGACAATGATCCAGGCCAGGAATCCATAACAC-3'
ZBRK1-as-NotI	5'-TATAGCGGCGCCTATGGGTTTTCTGTAACATAAAAATA-3'
qPCR-ChIP-IL4-FW	5'-CAAGATGCCACCTGTACTTGGA-3'
qPCR-ChIP-IL4-RV	5'-CCACAGGTGTCGAATTTGTT-3'
qPCR-ChIPZBS1-2-FW	5'-GGATCCGCCTTCTCAAG-3'
qPCR-ChIP-ZBS1-2-RV	5'-AAGAAATGCTTCTCCTGTCC-3'
qPCR-ChIP-ZBS3-FW	5' GCGGAGAATGTGTCTTGCTA 3'
qPCR-ChIP-ZBS3-RV	5'-ACTGGAGCGCTACTGTGTG-3'
qPCR-ChIP-ZBS4-FW	5'-GCCACCCGGCCACCT-3'
qPCR-ChIP-ZBS4-RV	5'-CCTATCCGCACCTCCG-3'
pGL3-ATXN2-FW	5'-GGGGACAAGTTTGTACAAAAAAGCAGGCTAGGGTTTTGCAATGGTCCCTTGATCT-3'
pGL3-ATXN2-RV	5'-GGGGACCCTTTGTACAAGAAAGCTGGGTCTACCCGGATCCGCCTTCTCAAG-3'
pGL3-ATXN2-Exon1-FW	5'-GGGGACAAGTTTGTACAAAAAAGCAGGCTTTTGTCAATGGTCCCTTGATCTACTTTTTT-3'
pGL3-ATXN2-Exon1-RV	5'-GGGGACCCTTTGTACAAGAAAGCTGGGTGTGGGAGCGGAGGTGCGGATAG-3'

Co-immunoprecipitation experiments

Co-immunoprecipitation experiments were performed using Hek293T cells or HeLa nuclei (Santa Cruz). Hek293T cells were grown in 15 mm plates and transfected with 42 μ l of PEI and 25 μ g of vectors pTL-FLAG-ZBRK1 or pTL-FLAG as a control. Forty-eight hours after transfection, cells were washed in 1 \times PBS (phosphate-buffered saline pH 7.4), harvested and lysed in lysis buffer [1 \times PBS, 5 mM EDTA (ethylenediaminetetraacetic acid), 0.5% Triton X-100, 2.5% protease inhibitor (complete tablets, Roche), 25 U/ml of benzamide (Merck)] for 45 min at 4°C. Afterwards, 0.75 μ g of mouse-ATXN2 antibody (BD Biosciences) were added to 1 mg of each cell lysate and incubated for 90 min on a rotating wheel at 4°C. Subsequently, 20.1 \times 10⁵ beads of sheep anti-mouse IgG Dynabeads M-280 (Invitrogen) were added and lysates were further incubated for 3 h. For experiments using HeLa nuclei, 1 μ g of mouse-ZBRK1 antibody (gift from Wen-Hwa Lee, University of California, Irvine, USA) was added to 250 μ g of nuclei extract. After incubation of samples for 3 h on a rotating wheel at 4°C, 10.05 \times 10⁵ beads of sheep anti-mouse IgG Dynabeads M-280 (Invitrogen) were added and the samples were incubated for an additional hour at 4°C. Dynabeads were pulled down magnetically and washed three times with 3% BSA (bovine serum albumin)/PBS and three times with PBS. To separate proteins from magnetic beads, 5 \times SDS sample buffer was added to samples and incubated for 5 min at 95°C. Proteins were separated by 7.5% SDS-PAGE and transferred to nitrocellulose membrane (Protran, Perkin Elmer) using a Perfect Blue semidry electroblotter (PeqLAB). Membranes were incubated in blocking solution (5% milk in 1 \times PBS) for 1 h at room temperature (RT), washed with PBS and incubated overnight with the respective primary antibody at 4°C [1:100, rabbit-ZBRK1 antibody (ATLAS antibodies); 1:1000, rabbit-ZBRK1 antibody (Abcam); 1:1000 mouse-ZBRK1 antibody (gift from Wen-Hwa Lee); 1:1000 mouse-ATXN2 antibody (BD Biosciences); 1:500, rabbit-ATXN2 antibody (Bethyl); 1:1000, rabbit-MYC antibody (Sigma-Aldrich); 1:5000, rabbit-FLAG antibody (Sigma-Aldrich); 1:5000, mouse-FLAG antibody (Sigma-Aldrich)]. Next, membranes were washed and incubated with the corresponding secondary peroxidase-coupled or alkaline phosphatase-coupled antibody

[mouse-POD-conjugate or rabbit-POD-conjugate, 1:10 000 (Sigma-Aldrich); goat-AP-conjugate and mouse-AP-conjugate, 1:10 000 (Jackson ImmunoResearch Laboratories)] for 2 h at RT. To visualize proteins, membranes were treated with Western Lightning luminol reagent (PerkinElmer) or SuperSignal West Femto (Thermo Scientific) and exposed to Amersham Hyperfilm ECL (Kodak). Membranes incubated with secondary alkaline phosphatase-coupled antibody were treated with Western Blue® (Promega).

Bioinformatic analysis

A search for ZBRK1-binding motifs within the *SCA2* promoter was performed using the SELEX-derived ZBRK1-binding motif described by Zheng *et al.* (4). For this, a scan for matches to the IUPAC string GGGnnnCAGnnnTTT was performed allowing for up to three mismatches restricted to the outer nucleotide triplets. The genomic sequence around the TSS of the *SCA2* gene as annotated in Ensembl v. 46, comprising 500 bp upstream and 300 bp downstream of the TSS, was extracted (29).

ChIP experiments

ChIP experiments were carried out as described previously (30). MCF-7 cells were lysed, nuclei were isolated and genomic DNA was sonicated to an average size of 400–800 bp. Shared samples were incubated overnight with 10 μ g of the respective antibody [rabbit-ZBRK1 antibody (Abcam), mouse-ATXN2 antibody (BD Biosciences)] and precipitated with Protein A Dynabeads (Invitrogen). Enrichment of potential ZBRK1-binding motifs within the analyzed *SCA2* sequence region was analyzed with RT-qPCR. Primers used in these experiments are listed in Table 1.

Quantitative real-time PCR

qPCR and RT-qPCR were applied to monitor genomic fragments or mRNA levels in colorectal cancers tissues, respectively. For the cDNA synthesis of a normal tumor mRNA, 30–300 ng of total RNA was reverse-transcribed with oligo-dT primers and SuperScriptII reverse transcriptase

(Invitrogen) in a 20 μ l reaction. qPCRs were performed in triplicates using Absolute SYBR Green PCR Master Mix (Applied Biosystems) in a 10 μ l reaction volume on a PRISM 7900HT sequence detection system (Applied Biosystems). The predicted threshold cycle (Ct) values and the amplification plot were obtained with the Sequence Detection software (SDS 2.1, Applied Biosystems). The housekeeping gene *HPRT1* (Hypoxanthine-guanine phosphoribosyltransferase) was used as the internal control, since it represents the best single reference gene for the standardization of gene expression measurements in cancer research (31).

Fold change was calculated with the $\Delta\Delta$ Ct method (User Bulletin #2, Applied Biosystems). Primers used are listed in Table 1.

Luciferase promoter activity assay

For promoter activity assays, Hek293T cells were plated in 96-well plates and transfected with 3 μ l of PEI and 50 ng of plasmid pGL3-ATXN2 or pGL3-ATXN2-Exon1, respectively, 5 ng of plasmid pRL-TK-Renilla and 100 ng of plasmids pCMV-HA-ZBRK1 or pCMV-MYC-ATXN2-Q22 or control vectors, respectively. Thirty-six hours post-transfection, cells were lysed in 20 μ l 1 \times Passive Lysis Buffer (Promega) for 15 min at RT and lysates were transferred to 96-well clear bottom plates. *Firefly* and *Renilla* luciferase activities were measured using the Dual-Luciferase Reporter Assay (Promega E1910) in a Centro LB960 luminometer (Berthold). Afterwards, *Firefly* luciferase activity was normalized to *Renilla* luciferase activity and ratios were set in relation to pGL3basic.

RNA interference experiments

RNA interference experiments were performed using Hek293T cells. For transfection, 30 000 cells were plated in a 12-well plate and transfected with HiPerfect (Qiagen) and 300 ng of the following small interfering RNA (siRNA) molecules: si-ZBRK1 (*On Target smart pool human ZNF350*, Dharmacon), si-ATXN2 (*On Target smart pool human SCA2*, Dharmacon) or si-NS (*On Target plus, non-targeting siRNA*, Dharmacon) as a control. Ninety-six hours post-transfection, cells were either lysed in lysis buffer [1 \times PBS, 5 mM EDTA, 0.5% Triton X-100, 2.5% protease inhibitor (complete tablets, Roche), 25 U/ml of benzonase (Merck)] for 45 min at 4°C or harvested for total RNA extraction using RNAeasy mini kit (Qiagen).

Confocal microscopy

U2OS and HeLa cells plated on glass slides were transfected with 3.3 μ l PEI and 1 μ g DNA of the corresponding plasmids and incubated for 16 h to allow transient expression of proteins. Cells were fixed with ice-cold methanol for at least 45 min and treated with 3% BSA. Subsequently, cells were incubated with primary antibodies (ATXN2, 1:200; BD Biosciences), FLAG (mouse and rabbit, 1:500; Sigma-Aldrich) for 1 h at RT, washed and incubated with respective secondary antibodies (mouse-AlexaFluor488, 1:500; Molecular Probes), rabbit-AlexaFluor568 (1:500;

Molecular Probes). Afterwards, samples were mounted with Fluoromount-G (SouthernBiotech) and analyzed by confocal microscopy using an LSM700 (Zeiss).

Generation of interfering intrabodies

The generation of intrabodies comprises an *in vitro* and an *in vivo* screening step applying phage display and a modified Y2H screen, respectively (Konthur *et al.*, manuscript in preparation). Briefly, potentially binding single-chain Fragment variables (scFv) were enriched *in vitro* from the human single-fold scFv library I (32). As selection target, the ZBRK1-CT was recombinantly expressed as *in vivo* biotinylated protein in *Escherichia coli* using the vector pRSET-BH6, where it was cloned via *Sall/NotI* as described above. Panning was carried out in solution applying a semi-automated selection protocol using magnetic beads in a magnetic particle processor as described before (33,34). Next, the enriched pools of scFvs were PCR amplified from the individual selection rounds using primers VH-tom-NcoI-f and VL-tom-NotI-rev, digested with the restriction endonucleases *NcoI/NotI* and subcloned into the *NcoI/NotI* restriction sites of the yeast expression vector pIB-NLS. For the *in vivo*-selection screening of intrabodies, the yeast strain L40ccuA/ade was generated and used. In brief, strain L40ccuA/ade expressing fusion proteins LexA-ATXN2-NT221–396 and AD-ZBRK1-CT was transformed with an intrabody library selected for ZBRK1-CT or with an unselected intrabody library as a control. For each library, 1152 transformants were isolated and spotted onto selective SDIII and SDV media plates. Yeast clones that did not show growth on SDV medium were indicative of carrying an intrabody with interfering properties for the ATXN2/ZBRK1 interaction. Subsequently, intrabody plasmids were isolated from the respective yeast clones and re-transformed for validation. Finally, plasmid-DNA derived from positive validated yeast clones was used as the template for PCR using primers 5'scFv-HindIII-pFLAG and 3'scFv-pFLAG. scFv amplicons were digested with restriction endonucleases *HindIII/NotI* and subcloned into the restriction sites *HindIII/NotI* of the mammalian expression vector pFlagCMV5a-ccdB.

Intrabody interference

For intrabody expression in mammalian cells, transfection was performed with 2 μ g of the respective pFlagCMV5a expression construct. Forty-eight hours post-transfection, cells were lysed in lysis buffer (50 mM Tris-HCl pH 8.8, 100 mM NaCl, 5 mM MgCl₂, 0.5% NP-40, 1 mM EDTA). Proteins were separated by 4–12% Bis-Tris-Gel (NuPAGE Novex, Invitrogen) according to the manufacturer's instructions and electrophoretically transferred to nitrocellulose membrane (Hybond ECL, GE Healthcare). Afterwards, membranes were incubated in 1% Tween, 2% Blocking Grade Blocker solution (BioRad) for at least 1 h at RT, washed three times with PBS/0.1% Tween followed by incubation with the first antibody overnight at 4°C as described above.

Tissue samples

Human tissues (ethics committee application number, 20-066) obtained during surgery were immediately snap-frozen in liquid nitrogen and stored at -80°C until they were processed. Patients selected had advanced colorectal cancers and were classified pT2N0M1 or higher. From each patient, normal and matching tumor samples were collected. Cryosections (3 μm thick) were prepared and stained with hematoxylin and eosin to evaluate tumor cell content. Dissections were performed under the microscope to achieve a tumor cell content of more than 80%. RNA isolation was performed using the AllPrep DNA/RNA/Protein Mini Kit (Qiagen), according to the manufacturer's instructions, quantified and analyzed with the Bioanalyzer (Agilent).

ACKNOWLEDGEMENTS

We are grateful to Wen-Hwa Lee, University of California, Irvine, USA, for providing the antibody against ZBRK1. We would also like to thank R. Querfurth, H.-J. Warnatz, A. Wunderlich, J. Langner and C. R. Galiveti for their help with experimental settings.

Conflict of Interest statement. None declared.

FUNDING

This work was supported by the Max Planck Society, the Ataxia UK Foundation (to Z.K. and S.K.), the German Federal Ministry for Education and Research, BMBF (NGFNII, 01GR0427 to Z.K., 01GS08111 to M.R.S.), the International Research Training Group-Genomics and Systems Biology of Molecular Networks (to H.K.).

REFERENCES

- Bellefroid, E.J., Lecocq, P.J., Benhida, A., Poncelet, D.A., Belayew, A. and Martial, J.A. (1989) The human genome contains hundreds of genes coding for finger proteins of the Kruppel type. *DNA*, **8**, 377–387.
- Tadepally, H.D., Burger, G. and Aubry, M. (2008) Evolution of C2H2-zinc finger genes and subfamilies in mammals: species-specific duplication and loss of clusters, genes and effector domains. *BMC Evol. Biol.*, **8**, 176.
- Urrutia, R. (2003) KRAB-containing zinc-finger repressor proteins. *Genome Biol.*, **4**, 231.
- Zheng, L., Pan, H., Li, S., Flesken-Nikitin, A., Chen, P.L., Boyer, T.G. and Lee, W.H. (2000) Sequence-specific transcriptional corepressor function for BRCA1 through a novel zinc finger protein, ZBRK1. *Mol. Cell*, **6**, 757–768.
- Vissing, H., Meyer, W.K., Aagaard, L., Tommerup, N. and Thiesen, H.J. (1995) Repression of transcriptional activity by heterologous KRAB domains present in zinc finger proteins. *FEBS Lett.*, **369**, 153–157.
- Tan, W., Zheng, L., Lee, W.H. and Boyer, T.G. (2004) Functional dissection of transcription factor ZBRK1 reveals zinc fingers with dual roles in DNA-binding and BRCA1-dependent transcriptional repression. *J. Biol. Chem.*, **279**, 6576–6587.
- Tan, W., Kim, S. and Boyer, T.G. (2004) Tetrameric oligomerization mediates transcriptional repression by the BRCA1-dependent Kruppel-associated box-zinc finger protein ZBRK1. *J. Biol. Chem.*, **279**, 55153–55160.
- Yun, J. and Lee, W.H. (2003) Degradation of transcription repressor ZBRK1 through the ubiquitin–proteasome pathway relieves repression of Gadd45a upon DNA damage. *Mol. Cell Biol.*, **23**, 7305–7314.
- Furuta, S., Wang, J.M., Wei, S., Jeng, Y.M., Jiang, X., Gu, B., Chen, P.L., Lee, E.Y. and Lee, W.H. (2006) Removal of BRCA1/CtIP/ZBRK1 repressor complex on ANGI promoter leads to accelerated mammary tumor growth contributed by prominent vasculature. *Cancer Cell*, **10**, 13–24.
- Garcia, V., Dominguez, G., Garcia, J.M., Silva, J., Pena, C., Silva, J.M., Carcereny, E., Menendez, J., Espana, P. and Bonilla, F. (2004) Altered expression of the ZBRK1 gene in human breast carcinomas. *J. Pathol.*, **202**, 224–232.
- Garcia, V., Garcia, J.M., Pena, C., Silva, J., Dominguez, G., Rodriguez, R., Maximiano, C., Espinosa, R., Espana, P. and Bonilla, F. (2005) The GADD45, ZBRK1 and BRCA1 pathway: quantitative analysis of mRNA expression in colon carcinomas. *J. Pathol.*, **206**, 92–99.
- Lin, L.F., Chuang, C.H., Li, C.F., Liao, C.C., Cheng, C.P., Cheng, T.L., Shen, M.R., Tseng, J.T., Chang, W.C., Lee, W.H. *et al.* (2010) ZBRK1 acts as a metastatic suppressor by directly regulating MMP9 in cervical cancer. *Cancer Res.*, **70**, 192–201.
- Lastres-Becker, I., Rub, U. and Auburger, G. (2008) Spinocerebellar ataxia 2 (SCA2). *Cerebellum*, **7**, 115–124.
- Nonhoff, U., Ralser, M., Welzel, F., Piccini, I., Balzereit, D., Yaspo, M.L., Lehrach, H. and Krobitsch, S. (2007) Ataxin-2 interacts with the DEAD/H-box RNA helicase DDX6 and interferes with P-bodies and stress granules. *Mol. Biol. Cell*, **18**, 1385–1396.
- Nonis, D., Schmidt, M.H., van de Loo, S., Eich, F., Dikic, I., Nowock, J. and Auburger, G. (2008) Ataxin-2 associates with the endocytosis complex and affects EGF receptor trafficking. *Cell Signal.*, **20**, 1725–1739.
- Ralser, M., Albrecht, M., Nonhoff, U., Lengauer, T., Lehrach, H. and Krobitsch, S. (2005) An integrative approach to gain insights into the cellular function of human ataxin-2. *J. Mol. Biol.*, **346**, 203–214.
- Ralser, M., Nonhoff, U., Albrecht, M., Lengauer, T., Wanker, E.E., Lehrach, H. and Krobitsch, S. (2005) Ataxin-2 and huntingtin interact with endophilin-A complexes to function in plastin-associated pathways. *Hum. Mol. Genet.*, **14**, 2893–2909.
- Aprelikova, O., Pace, A.J., Fang, B., Koller, B.H. and Liu, E.T. (2001) BRCA1 is a selective co-activator of 14–3–3 sigma gene transcription in mouse embryonic stem cells. *J. Biol. Chem.*, **276**, 25647–25650.
- Harkin, D.P., Bean, J.M., Miklos, D., Song, Y.H., Truong, V.B., Englert, C., Christians, F.C., Ellisen, L.W., Maheswaran, S., Oliner, J.D. *et al.* (1999) Induction of GADD45 and JNK/SAPK-dependent apoptosis following inducible expression of BRCA1. *Cell*, **97**, 575–586.
- MacLachlan, T.K., Somasundaram, K., Sgagias, M., Shifman, Y., Muschel, R.J., Cowan, K.H. and El-Deiry, W.S. (2000) BRCA1 effects on the cell cycle and the DNA damage response are linked to altered gene expression. *J. Biol. Chem.*, **275**, 2777–2785.
- Welsh, P.L., Lee, M.K., Gonzalez-Hernandez, R.M., Black, D.J., Mahadevappa, M., Swisher, E.M., Warrington, J.A. and King, M.C. (2002) BRCA1 transcriptionally regulates genes involved in breast tumorigenesis. *Proc. Natl Acad. Sci. USA*, **99**, 7560–7565.
- Frietze, S., Lan, X., Jin, V.X. and Farnham, P.J. (2010) Genomic targets of the KRAB and SCAN domain-containing zinc finger protein 263. *J. Biol. Chem.*, **285**, 1393–1403.
- Wiedemeyer, R., Westermann, F., Wittke, I., Nowock, J. and Schwab, M. (2003) Ataxin-2 promotes apoptosis of human neuroblastoma cells. *Oncogene*, **22**, 401–411.
- Reddy, P.S. and Housman, D.E. (1997) The complex pathology of trinucleotide repeats. *Curr. Opin. Cell Biol.*, **9**, 364–372.
- Schols, L., Bauer, P., Schmidt, T., Schulte, T. and Riess, O. (2004) Autosomal dominant cerebellar ataxias: clinical features, genetics, and pathogenesis. *Lancet Neurol.*, **3**, 291–304.
- Stevanin, G., Durr, A. and Brice, A. (2002) Spinocerebellar ataxias caused by polyglutamine expansions. *Adv. Exp. Med. Biol.*, **516**, 47–77.
- Huynh, D.P., Del Bigio, M.R., Ho, D.H. and Pulst, S.M. (1999) Expression of ataxin-2 in brains from normal individuals and patients with Alzheimer's disease and spinocerebellar ataxia 2. *Ann. Neurol.*, **45**, 232–241.
- Goehler, H., Lalowski, M., Stelzl, U., Waelter, S., Stroedicke, M., Worm, U., Droege, A., Lindenberg, K.S., Knoblich, M., Haenig, C. *et al.* (2004) A protein interaction network links GIT1, an enhancer of huntingtin aggregation, to Huntington's disease. *Mol. Cell*, **15**, 853–865.
- Flicek, P., Aken, B.L., Ballester, B., Beal, K., Bragin, E., Brent, S., Chen, Y., Clapham, P., Coates, G., Fairley, S. *et al.* (2010) Ensembl's 10th year. *Nucleic Acids Res.*, **38**, D557–562.

30. Sultan, M., Schulz, M.H., Richard, H., Magen, A., Klingenhoff, A., Scherf, M., Seifert, M., Borodina, T., Soldatov, A., Parkhomchuk, D. *et al.* (2008) A global view of gene activity and alternative splicing by deep sequencing of the human transcriptome. *Science*, **321**, 956–960.
31. de Kok, J.B., Roelofs, R.W., Giesendorf, B.A., Pennings, J.L., Waas, E.T., Feuth, T., Swinkels, D.W. and Span, P.N. (2005) Normalization of gene expression measurements in tumor tissues: comparison of 13 endogenous control genes. *Lab. Invest.*, **85**, 154–159.
32. Holt, L.J., Bussow, K., Walter, G. and Tomlinson, I.M. (2000) By-passing selection: direct screening for antibody–antigen interactions using protein arrays. *Nucleic Acids Res.*, **28**, E72.
33. Rhyner, C., Konthur, Z., Blaser, K. and Cramer, R. (2003) High-throughput isolation of recombinant antibodies against recombinant allergens. *Biotechniques*, **35**, 672–674.
34. Walter, G., Konthur, Z. and Lehrach, H. (2001) High-throughput screening of surface displayed gene products. *Comb. Chem. High Throughput Screen.*, **4**, 193–205.
35. Rhead, B., Karolchik, D., Kuhn, R.M., Hinrichs, A.S., Zweig, A.S., Fujita, P.A., Diekhans, M., Smith, K.E., Rosenbloom, K.R., Raney, B.J. *et al.* (2010) The UCSC Genome Browser database: update 2010. *Nucleic Acids Res.*, **38**, D613–619.
36. Gardiner-Garden, M. and Frommer, M. (1987) CpG islands in vertebrate genomes. *J. Mol. Biol.*, **196**, 261–282.